

# Plasma Temperature Inference from DT/DD Neutron Discrimination

J. I. Katz\*

Los Alamos National Laboratory

P. O. Box 1663, Los Alamos, N. Mex. 87545

and

Department of Physics

and

McDonnell Center for the Space Sciences

Washington University, St. Louis, Mo. 63130

April 1, 2024

---

\*Proofs to: J. I. Katz, Department of Physics, CB1105, Washington University, 1 Brookings Dr., St. Louis, Mo. 63130. 19 pp., 3 figures, 1 table [katz@wuphys.wustl.edu](mailto:katz@wuphys.wustl.edu)  
facs: 314-935-6219

# Plasma Temperature Inference from DT/DD Neutron Discrimination

J. I. Katz

## Abstract

DD and DT reaction rates may be compared to determine plasma temperatures in the 10–200 eV range. Distinguishing neutrons from these two reactions is difficult when yields are low or unpredictable. Time of flight methods fail if the source is extended in time. These neutrons may be distinguished because inelastic scattering of more energetic neutrons by carbon produces a 4.44 MeV gamma-ray, and because hydrogenous material preferentially attenuates lower energy neutrons. We describe a detector system that can discriminate between lower and higher energy neutrons for fluences as low as  $\mathcal{O}(10^2)$  neutrons/sterad even when time of flight methods fail, define a figure of merit and calculate its performance over a broad range of parameters.

Keywords: Neutron energy discrimination; plasma temperature

# I Introduction

Plasma temperatures in the range 10–200 eV can be difficult to measure because at those temperatures thermal emission is in the vacuum UV and soft X-ray bands and is strongly absorbed by matter. This problem is acute if the plasma is surrounded by cold dense matter. For example, opaque cold dense metallic imploding liners may be used to compress and heat plasmas, with the ultimate goal of thermonuclear fusion [1].

We consider the problem of measuring plasma temperatures in the approximate range 10—200 eV if radiation from the plasma is not directly observable. At these temperatures the very soft X-rays of thermal emission are strongly absorbed by most substances (including vacuum windows, for example), so that this circumstance may be frequently encountered. If the plasma contains a suitable admixture of deuterium and tritium, comparison of the rate of the  $D(D, {}^3\text{He})n$  reaction, producing 2.45 MeV neutrons, to that of the  $D(T, \alpha)n$  reaction, producing 14.1 MeV neutrons, may permit the determination of the temperature.

The ratio of these reaction rates is significantly dependent on temperature. The steep increase of both reaction rates with increasing temperature in this regime implies that the temperature determined is that of the highest temperature encountered in the system, even though that may be found in only a small fraction of its volume. It is also insensitive to other parameters such as the volume and density at peak temperature and the confinement

time.

Determining plasma temperature by comparison of DD and DT reactions in this low temperature regime involves some special problems. Because of the extreme sensitivity of the reaction rates to temperature, the total number of neutrons produced may be small. In addition, it may not be predictable even in order of magnitude because small uncertainties in the temperature correspond to great uncertainties in the reaction rates. The small number of expected neutrons requires that detectors be close to the source, and sources produced by, for example, comparatively massive imploding liners may have long lifetimes. For these reasons the usual method of discriminating neutrons of different energy, their times of flight, may not be feasible. After examining this issue, this paper discusses other methods. Discrimination based on the ability of the more energetic DT neutrons to excite the 4.44 MeV state of  $^{12}\text{C}$  and on the greater elastic scattering cross-section of lower energy neutrons in hydrogen may be the most feasible method. A detector design is outlined, a figure of merit defined, and quantitative simulation results are presented.

Because this method depends on the thermonuclear reaction rates, these are shown in Figure 1 for  $k_B T < 25$  keV. At these temperatures the non-resonant expressions given by [2] are valid, and the Figure extends to lower temperatures than are usually shown. It is also necessary to include the effects of electron screening [3], which increases the reaction rates at the lowest temperatures considered by several orders of magnitude at high, but plausible, densities.

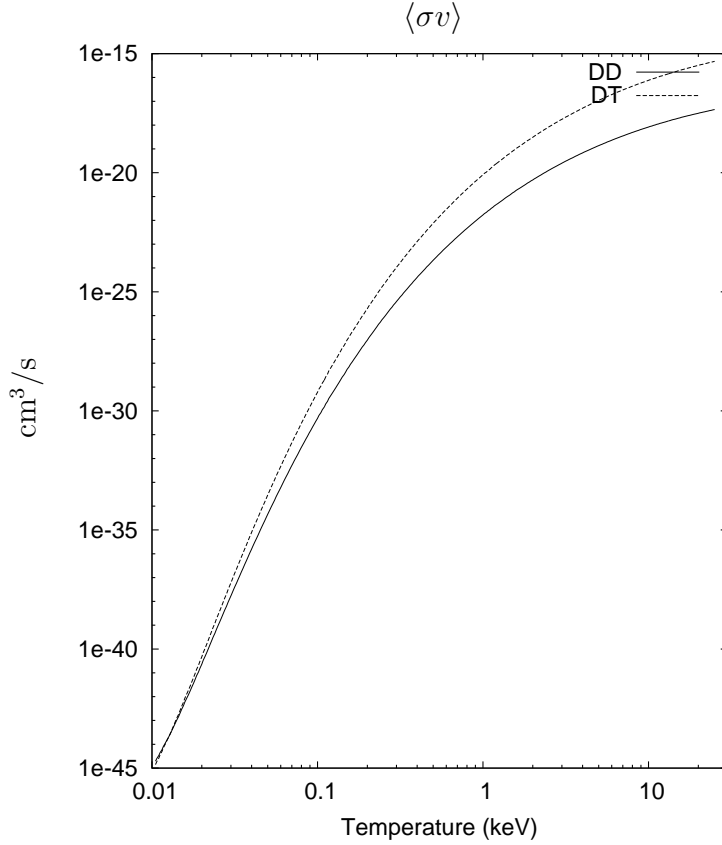


Figure 1: Maxwell-averaged reaction rate coefficients [2], showing their steep dependence on temperature at low temperature. Electron shielding [3] in weak and intermediate regimes is included for an assumed density of  $100 \text{ gm/cm}^3$ , as in some inertial fusion targets.

Figure 2 shows the ratio of the DT to the DD reaction rates and the logarithmic derivative  $\partial \ln \langle\sigma v\rangle / \partial \ln T$  of the DT reaction rate with respect to temperature (the result for the DD rate is very similar). For comparatively low ( $\lesssim 200 \text{ eV}$ ) temperatures the ratio of the fluence of DT to DD neutrons unambiguously determines the temperature in the reaction region,

independent of any other parameter, as shown in Fig. 2.

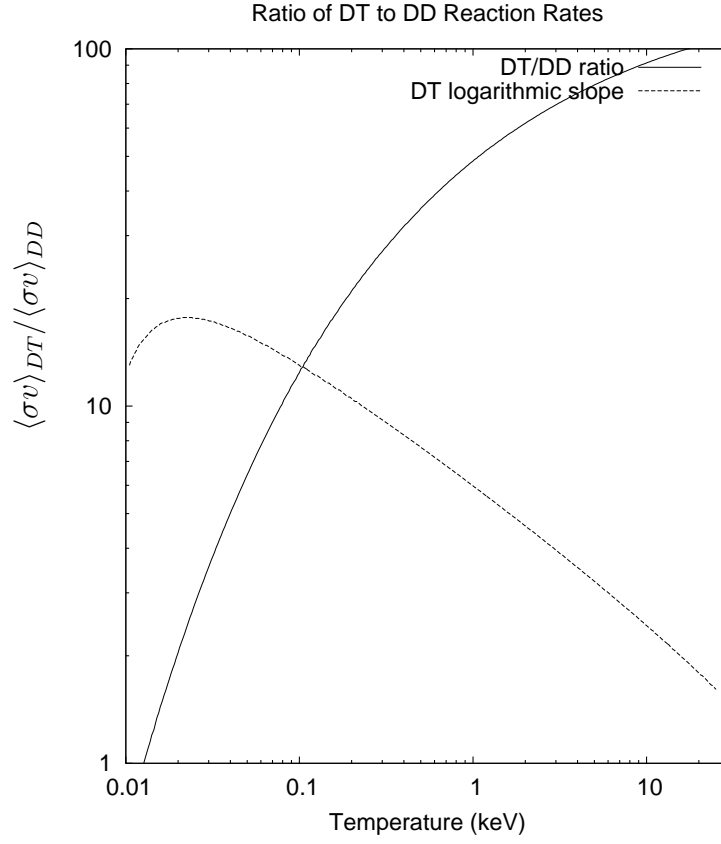


Figure 2: Ratio of DT to DD reaction rates and logarithmic derivative of the DT rate with respect to temperature.

## II Distinguishing DT from DD neutrons

### II.A Time of Flight

At low temperatures the number of neutrons produced is small. The usual method of determining source temperatures from the width of the arrival time distribution at a detector of neutrons produced by a single reaction is difficult or impossible, partly because the weak source requires a detector close to it, reducing the spread of arrival times, partly because low temperatures reduce that spread further, and most importantly because of the poor statistics when only a small number of neutrons are detected.

For example, at a distance of 1 m and a source temperature of 100 eV the  $1/e$  half-width of the arrival time distribution of DT neutrons is 23 ps, while that of DD neutrons is 147 ps. These widths are the flight times multiplied by  $\sqrt{2k_B T / M v_n^2} = \sqrt{k_B T / (E_n A)}$ , where  $M$  is the total mass of the reactants,  $v_n$  the neutron velocity,  $E_n$  the neutron energy and  $A$  the sum of the atomic numbers of the reactants. For the DT reaction this is 0.0012, while for the DD reaction it is 0.0032; if the source is distributed over a region whose size is this fraction of the distance to the detector (1.2 mm and 3.2 mm, respectively, for DT and DD reactions at 1 m distance) then the variation in path lengths will wash out any information about the source temperature obtainable from time of flight.

The difference in time of flight between 2.45 MeV (DD) and 14.1 MeV (DT) neutrons is much larger, and if both reactions occur might be used

to distinguish these two populations and to infer the temperature from the ratio of their reaction rates. At 1 m range the 14.1 MeV DT neutrons arrive after 19 ns, while the 2.45 MeV DD neutrons arrive after 46 ns, a lag of 27 ns. This interval is measurable with plastic scintillators whose response times may be 2–10 ns. However, separation by time of flight, even into 2.45 and 14.1 MeV energy groups, is possible only if the source duration is less than the interval between the arrivals of 14.1 MeV and 2.45 MeV neutrons. If the source duration is comparable to or greater than this interval, as in imploding liner experiments in which neutrons may be emitted over a time  $\gtrsim 100$  ns [1], another method of discrimination is required.

## II.B Energy Deposited

For sources with long ( $\gtrsim 30d$  ns) durations at a distance  $d$  (in m) discrimination of DT from DD neutrons is not possible by time of flight alone, even for an ideal detector. Discrimination on the basis of the energy deposited could be possible, provided the detector were segmented so that  $\lesssim 1$  neutron interacts in each segment. This would require  $\gtrsim N$  segments, where  $N$  is the total number of detected neutrons. If the fluences were approximately predictable, the segment sizes could be chosen to keep  $N$  in a feasible range.

To determine the ratio of DT to DD neutrons to a fractional accuracy  $f$  at  $s$  standard deviations significance, for the optimal case in which this ratio

is  $\approx 1$ , requires

$$N \gtrsim \frac{4s^2}{f^2}. \quad (1)$$

For  $f = 0.1$  (even though the reaction rates are very sensitive to temperature their ratio is not) and  $s = 2$  we find  $N > 1600$ . The number of discrete segments must be comparable (the large ratio of energy between the two neutron groups permits some discrimination even when two or three neutrons are detected in a single segment).

This might be feasible (if the plastic scintillator were a bundle of fibers, each optically coupled to a single pixel in an imager that may have  $> 10^6$  pixels), provided that the flux is predictable to a factor of  $\mathcal{O}(1)$ . If not predictable, as is likely when source temperatures are low because of the extreme temperature sensitivity of the reaction rates, either too few neutrons would be detected for statistical significance or too many. In a segment in which  $\gtrsim 5$  MeV is deposited it would not be possible to distinguish a number of 14.1 MeV neutrons from several times that number of 2.45 MeV neutrons.

## II.C Activation

DT neutrons may activate nuclei that cannot be activated by the lower energy DD neutrons. A promising candidate, on account of its cross-section, half-life and detectability of the product, is the  $^{27}\text{Al}(n,\alpha)^{24}\text{Na}$  reaction with a threshold of 3.25 MeV. Detection would require rapid processing (the half-life of  $^{24}\text{Na}$  is only 15 hours, while those of most other candidate targets are

even shorter) of large quantities of material.

The cross-section for this reaction at 14.1 MeV is about 0.12 b, while the total scattering cross section is about 1.75 b and inelastic scattering ( $^{27}\text{Al}$  has low-lying states at 0.844 MeV and 1.014 MeV and many more states above 2 MeV) has a cross-section of about 0.4 b at 14.1 MeV, and somewhat greater at energies between 2 and 10 MeV. In a thick Al slab the fraction of incident neutrons producing activation is no more than 10%; even though energy loss by recoil in elastic scattering is small (roughly 1/27 of the neutron's incident energy), energetic neutrons lose energy rapidly by inelastic scattering. A thick slab must have a column density  $> 25 \text{ g/cm}^2$  (thickness  $> 10 \text{ cm}$ ), a mass of hundreds of kg for a 1 sterad activation target at a distance of 1 m from the source. The total activation efficiency, allowing for solid angle and the cross-sections, is then  $\lesssim 1\%$ . This massive slab of Al must be dissolved and a handful of  $^{24}\text{Na}$  nuclei efficiently separated (perhaps by reprecipitation of the Al and extraction of Na from the supernatant) in a few hours, and their decay gamma rays efficiently counted. Although a conceivable means of detecting yields  $> 10^3$  of DT neutrons, and of measuring yields  $> 10^4\text{--}10^5$  neutrons with useful accuracy, this would be cumbersome.

## II.D Inelastic scattering

DT neutrons (14.1 MeV) may produce prompt  $\gamma$ -rays by inelastic scattering to levels that cannot be reached by scattering of the 2.45 MeV neutrons of DD reactions. Carbon is a uniquely favorable target because both its stable

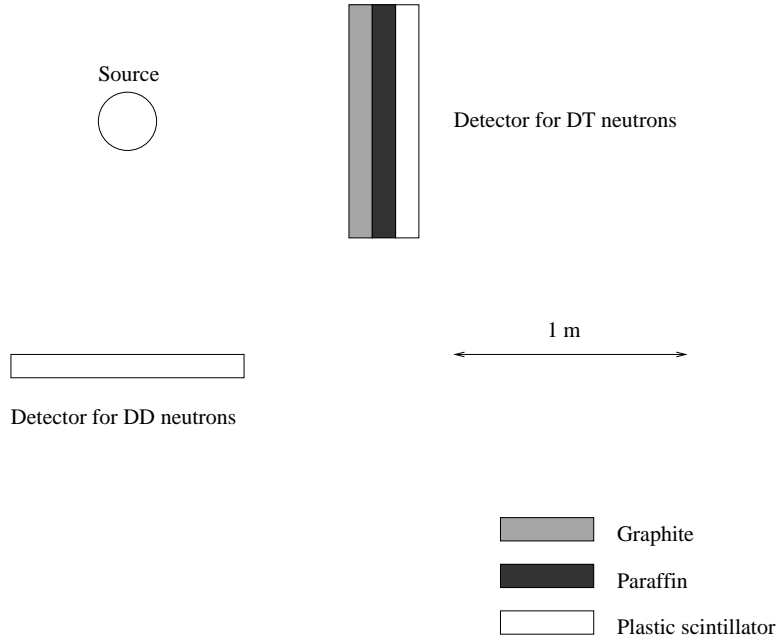


Figure 3: Detector system, approximately to scale, to measure and distinguish DT and DD neutrons from a weak neutron source.

isotopes have thresholds for excitation above 2.45 MeV (for other elements, even oxygen, some isotope has a lower excitation threshold) and for its ready availability and convenience. A scintillator shielded by hydrogenous material would detect the  $\gamma$ -rays.

A possible design is shown in Fig. 3. The first slab (closest to the source) is made of graphite. For a 14.1 MeV neutron the cross-section  $\sigma_{n,\gamma}$  for excitation of the first excited state, which is followed by emission of a 4.44 MeV  $\gamma$ -ray, is 0.21 b. This process competes with the total cross-section  $\sigma_t$  of 1.32 b. Neutron transport is complicated, but for the purposes of an analytic estimate we make the (conservative) approximation that the incident

neutron flux is exponentially attenuated at the rate  $\beta \equiv n_C \sigma_t = 0.145/\text{cm}$ , where for a graphite density of  $2.16 \text{ gm/cm}^3$   $n_C = 1.1 \times 10^{23} \text{ cm}^{-3}$ . This ignores excitation by scattered neutrons, whose energy remains well above the excitation threshold even after  $\mathcal{O}(10)$  elastic scatterings ( $\sigma_{n,\gamma}$  is roughly constant in the range 6–14 MeV), although inelastic scattering into the  $3\alpha$  channel at energies above 7.89 MeV, included in  $\sigma_t$ , reduces the excitation by scattered neutrons.

The neutron to gamma-ray conversion rate  $\gamma \equiv n_C \sigma_{n,\gamma} = 0.23/\text{cm}$ , and 4.44 MeV gamma rays are attenuated in graphite at a rate  $\alpha \equiv n_C \sigma_{abs} = 0.063/\text{cm}$  ( $\sigma_{abs} = 0.57 \text{ b}$ , essentially the Compton scattering cross-section). We make a one-stream approximation but allow for the fact that half of the emitted gamma rays are directed backwards by using  $\gamma' = \gamma/2$ , and take the attenuation coefficient for gamma rays at the mean angle to the normal of an isotropic distribution ( $60^\circ$ ):  $\alpha' = 2\alpha$ . The latter approximation is conservative because attenuation collimates the gamma ray flux into small angles to the slab normals with an effective attenuation coefficient close to  $\alpha$  rather than  $\alpha'$ . The gamma ray flux at a depth  $z$  into the graphite slab

$$f_\gamma = \frac{f_{DT}\gamma'}{\alpha' - \beta} [\exp(-\beta z) - \exp(-\alpha' z)], \quad (2)$$

where  $f_{DT}$  is the incident 14.1 MeV neutron flux. This is maximized at a

depth, corresponding to the optimal slab thickness,

$$z_{opt} = \frac{\ln(\beta/\alpha')}{\beta - \alpha'} = 7.4 \text{ cm} \approx \frac{1}{\beta}. \quad (3)$$

The emergent 4.44 MeV  $\gamma$ -ray flux, in this approximation, is

$$\begin{aligned} f_{\gamma} &= f_{DT} \frac{\gamma'}{\alpha' - \beta} [\exp(-\beta z_{opt}) - \exp(-\alpha' z_{opt})] \\ &= f_{DT} \frac{\gamma'}{\alpha' - \beta} \left[ \left( \frac{\beta}{\alpha'} \right)^{-\beta/(\beta-\alpha')} - \left( \frac{\beta}{\alpha'} \right)^{-\alpha'/(\beta-\alpha')} \right] \\ &= 0.031 f_{DT}. \end{aligned} \quad (4)$$

A 1 m<sup>2</sup> slab (about 1 sterad at 1 m distance), 7.4 cm thick, of graphite has a mass of 160 kg. It need not be high purity, and (unlike an aluminum activation target) may be reused indefinitely without processing.

## II.E Filtering

Graphite has a scattering cross section to 2.45 MeV neutrons of 1.59 b, so that their unscattered flux is attenuated at a rate  $\beta_{DD} = 0.175/\text{cm}$  and the flux that emerges unscattered from a slab of thickness  $z_{opt}$  is

$$f_{2.45} = f_{DD} \exp(-\beta_{DD} z_{opt}) = 0.27 f_{DD}. \quad (5)$$

This compares unfavorably with the 4.44 MeV  $\gamma$ -ray flux Eq. 4, and it is necessary to attenuate the lower energy neutrons.

These can be attenuated by a slab of hydrogenous material such as paraffin wax or polyethylene, as shown in Fig. 3. Because of the large neutron scattering cross-section of hydrogen at 2.45 MeV (2.6 b), the total cross-section of wax per carbon atom is 6.8 b, and at a density of 0.9 g/cm<sup>3</sup> the unscattered 2.45 MeV neutron flux is attenuated at a rate of 0.26/cm. In contrast, the cross-section of wax per carbon atom for 4.44 MeV *photons* is only 0.76 b, and they are attenuated at a rate of 0.060/cm, where we have again taken a mean angle to the normal of 60°. The scattering cross-section of wax for 14.1 MeV neutrons is 2.66 b per carbon, and the attenuation is 0.10/cm.

A thickness of 10 cm of wax attenuates the unscattered 2.45 MeV neutrons by a factor of 0.074, but the 4.44 MeV gamma rays by a factor of 0.55. The resulting flux ratio, using Eqs. 4 and 5,

$$\frac{f_{\gamma}}{f_{2.45}} = \frac{0.55}{0.074} \frac{0.031 f_{DT}}{0.27 f_{DD}} = 0.85 \frac{f_{DT}}{f_{DD}}. \quad (6)$$

Each additional 10 cm of paraffin multiplies the coefficient in Eq. 6 by a factor of  $0.55/0.074 = 7.4$  while reducing the  $\gamma$ -ray sensitivity by only 45%, so that a thick sandwich detector is effectively only sensitive to 14.1 MeV neutrons and the gamma-rays they produce.

## II.F Data Inversion

DD neutrons may be detected by a simple scintillator detector. The more energetic DT neutrons and the gamma rays they produce will also excite the scintillator, so it produces a weighted sum signal. Once calibrated, the fluxes of the two energies of neutrons may be found from the signals in the two scintillators by inverting the response matrix  $\mathbf{R}$ . This matrix is defined by the relation between the numbers  $N_i$  of source neutrons and the energies  $E_i$  deposited in the  $i$ -th detector:

$$\begin{pmatrix} E_1 \\ E_2 \end{pmatrix} = \begin{pmatrix} r_{11} & r_{12} \\ r_{21} & r_{22} \end{pmatrix} \begin{pmatrix} N_1 \\ N_2 \end{pmatrix}, \quad (7)$$

where  $i = 1$  denotes 14.1 MeV neutrons and the unfiltered scintillator, and  $i = 2$  denotes 2.45 MeV neutrons and the filtered detector.

## III Quantitative Results

We use the Monte-Carlo simulation code MCNP6 to calculate the energy deposited in the scintillators in the detector geometry of Fig. 3 when subjected to fluences of 2.45 and 14.1 MeV neutrons. The slabs are circular discs 1 m in diameter, and the centers of the closest surfaces of each detector array are 1 m from a point neutron source at the origin, so that the front surfaces of each detector subtend a solid angle 0.663 sterad at the neutron source, or 0.0528 of the sphere. The calculation includes all relevant neutron, electron

and photon processes.

We define a figure of merit of the detector system:

$$\text{FOM} \equiv \frac{r_{21}}{r_{22}} \frac{r_{12}}{r_{11}}. \quad (8)$$

The first factor is the ratio of energy deposited by 2.45 MeV neutrons into the unfiltered detector to that deposited into the detector with graphite converter and filter, and the second factor is the ratio of energy deposited by 14.1 MeV neutrons into the detector with converter and filter to that deposited into the unfiltered detector. Ideally, these ratios would be infinite, so that the unfiltered detector would only detect 2.45 MeV neutrons and the detector with converter and filter would only detect 14.1 MeV neutrons. Conversely, if the two detectors had the same response to neutrons of each energy the factors would be unity,  $\mathbf{R}$  would be singular,  $\text{FOM} = 1$  and it would be impossible to determine the separate production rates of 2.45 MeV and 14.1 MeV neutrons.

The accuracy with which the neutron sources can be inferred from the data is limited by statistical uncertainty in the energy deposited in the scintillators because of the finite number of deposition events. The system maximizes FOM by heavily filtering the flux in detector 2, reducing the energy deposited and increasing its statistical uncertainty. The optimum choice of detector parameters requires a tradeoff among these criteria and other factors such as cost.

	graphite	paraffin	scintillator	FOM	$\sigma_2\sqrt{N_1}/10^4$
1	10	10	10	2.25	0.089
2	5	5	10	1.69	0.063
3	2	2	10	1.25	0.054
4	1	1	10	1.11	0.047
5	15	15	10	2.53	0.123
6	20	20	10	2.57	0.168
7	20	10	10	2.28	0.123
8	10	15	10	2.53	0.104
9	10	20	10	2.68	0.120
10	10	25	10	2.72	0.142
11	10	10	5	2.21	0.092
12	10	10	20	2.38	0.092
13	0	10	10	1.89	0.047

Table I: Detector performance. The first three columns indicate the thicknesses (in cm) of the graphite neutron to gamma-ray converter and paraffin neutron filter for detector 2 and (for both detectors) the thickness of the plastic scintillator. FOM is the system figure of merit defined in Eq. 8. The final column shows the fractional statistical uncertainty in the energy deposited in the filtered detector 2 by 14.1 MeV neutrons and their products, the critical uncertainty in determining  $N_1/N_2$ ;  $\sigma_2 \propto N_1^{-1/2}$ . The calculational uncertainties in the FOM are about  $\pm 0.01$ .

Table I presents the results of model calculations. These results show that FOM increases only slowly with converter and filter thicknesses beyond 10 cm, but that increased thickness significantly increases the statistical uncertainty, so that values near 10 cm appear to be near optimal. Increasing the scintillator thickness in the baseline case (line 1) from 10 cm to 20 cm (line 12) increases the energy deposited in the filtered detector 2 by a source of 14.1 MeV neutrons by 60%, but does not reduce its statistical uncertainty.

The Monte-Carlo results also show that typically about 70% of the energy

deposition in the scintillator of detector 2 is by neutrons. The graphite turns a portion of the energy of 14.1 MeV neutrons into gamma rays, but it and the paraffin filter also function as a neutron energy discriminator, preferentially attenuating lower energy neutrons. Comparison of the baseline line 1 with line 13 in which the graphite is omitted shows that the graphite significantly increases the FOM, but that the paraffin filter alone discriminates between 14.1 MeV and 2.45 MeV neutrons.

Statistical uncertainties may be estimated from entries in the last column that show the fractional standard deviation  $\sigma_2$  of  $E_2$  (contributed by the 14.1 MeV neutron source that typically accounts for 80% of  $E_2$ ). The Monte Carlo simulations used  $N_1 = N_2 = 10^7$  to minimize simulation (as opposed to experimental) statistical uncertainty. The statistical uncertainty  $\sigma_1$  of  $E_1$  in the unfiltered detector is generally smaller because several times as much energy is deposited in it, so  $\sigma_2$  is a fair estimate of the fractional uncertainty in  $N_1$ . Because the 2.45 MeV neutrons principally contribute to  $E_1$  (with its smaller uncertainty) the fractional uncertainty in  $N_2$  will generally be smaller than that in  $N_1$ .

Although  $\sigma_2$  is only one contribution to uncertainty in the desired ratio  $N_1/N_2$ , provided  $\text{FOM} \gtrsim 2$  it is the dominant source of uncertainty. Hence, if  $N_1 \gtrsim 10^4$  and  $N_2 \gtrsim 10^4$  the ratio  $N_1/N_2$  may, with good choice of detector parameters, be determined to a  $1\sigma$  accuracy of better than 20%. At temperatures of a few tens of eV this corresponds to a comparable fractional uncertainty in temperature (the logarithmic slope of the solid line in

Fig. 2 is close to unity). Because of the extreme temperature sensitivity ( $\propto T^{15}$ ; Fig. 2) of both reaction rates in this temperature range, this implies a roughly ten-fold uncertainty in  $\int_{T \geq 0.93T_{max}} n^2 dV$ , where  $n$  is the particle density and the integral is taken over the region in which the temperature is within 7% of its maximum value. In this region the reaction rate is within a factor of three of its maximum, and the integral is a fair approximation to  $\int \langle \sigma v \rangle(T) n^2 dV / \langle \sigma v \rangle(T_{max})$ , a single parameter description of the reaction region.

I thank Carl Hagelberg for essential discussions. The Los Alamos National Laboratory is operated by Los Alamos National Security, LLC for the U. S. Department of Energy under Contract No. DE-AC52-06NA25396.

## References

- [1] Turchi, P. J., Imploding Liner Compression of Plasma: Concepts and Issues *IEEE Trans. Plasma Science* **36** (1), 52–61 DOI:10.1109/TPS.2007.914173 (2008).
- [2] Huba, J. D., *NRL Plasma Formulary*, Naval Research Laboratory, Washington, D. C. (2007).
- [3] Salpeter, E. E. and van Horn, H. M., Nuclear Reaction Rates at High Densities *Ap. J.* **155**, 183–202 (1969).